Supplementary Materials

Pengcheng Zhu,[1] *Zilong Guo*,*[,2], *Yulin Sha,*[1] *Yonghang Li,*[1] *Xiaoyu Zhang*[3], *Yangdong Han*[3], *and Wensheng Yang**[,1,3] *and Xiaonan Ma,*[1]

[1] Institute of Molecular Plus, Tianjin University, Tianjin 300072, P. R. China;

[2] School of Materials Science and Engineering, Changchun University of Science and Technology, Changchun 130022, P. R. China;

[3] Engineering Research Center for Nanomaterials, Henan University, Kaifeng 475004, P. R. China.

*zilong.guo@cust.edu.cn

*wsyang@hnu.edu.cn

Contents

Section	Content	Page
S1	Preparation and Characterization of Particles	S3
	Figure S1	S3
	Figure S2	S3
S2	Characterization of PdOEP-embedded silica particles	S4
	Figure S3	S4
	Figure S4	S5
	Table S1	S5
	Figure S5	S6
	Figure S6	S6
	Figure S7	S7
S3	Spectral characterization of particles and dependence on free volume	S8
	Figure S8	S8
	Figure S9	S8
S4	Experiment on the sensitizing ability of singlet oxygen	S8
	Figure S10	S9
	Figure S11	S10
	Figure S12	S10
	Figure S13	S11
	Figure S14	S11

Section S1. Preparation and Characterization of Particles

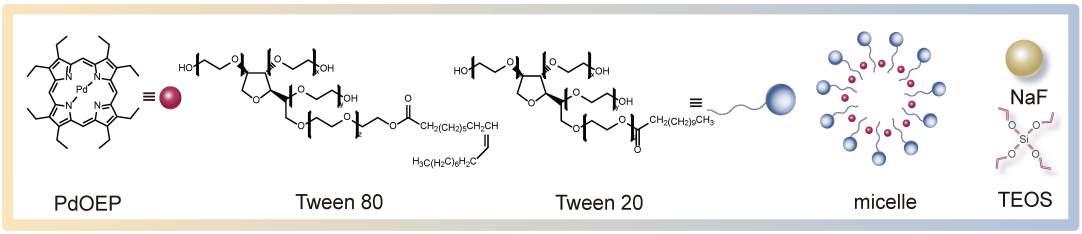


Figure S1. The chemical structure of the reagent used to prepare PdOEP-embedded silica particles.

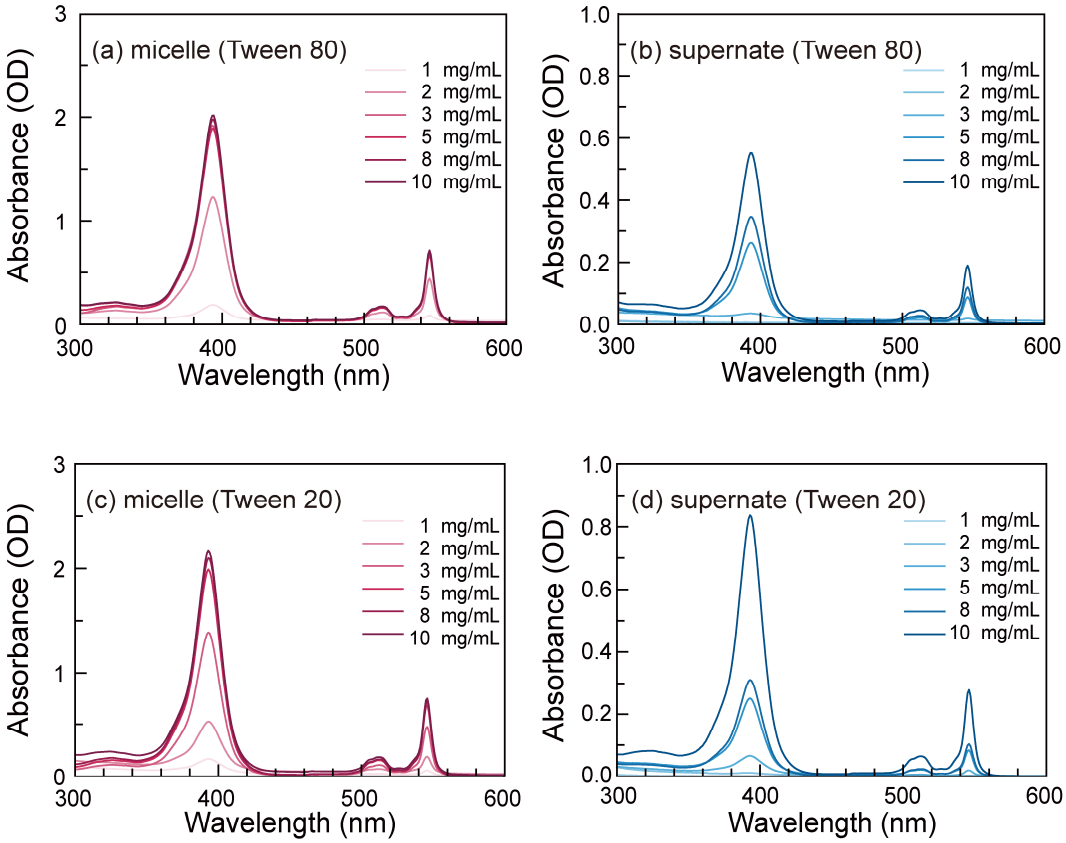


Figure S2. (a) and (b) are the absorbance spectra of the micelles prepared by Tween 80 and the absorption spectra of the supernate after centrifugation during the silica coating process, (c) and (d) are the analogous spectra obtained with Tween 20.

Section S2. Characterization of PdOEP-embedded silica particles

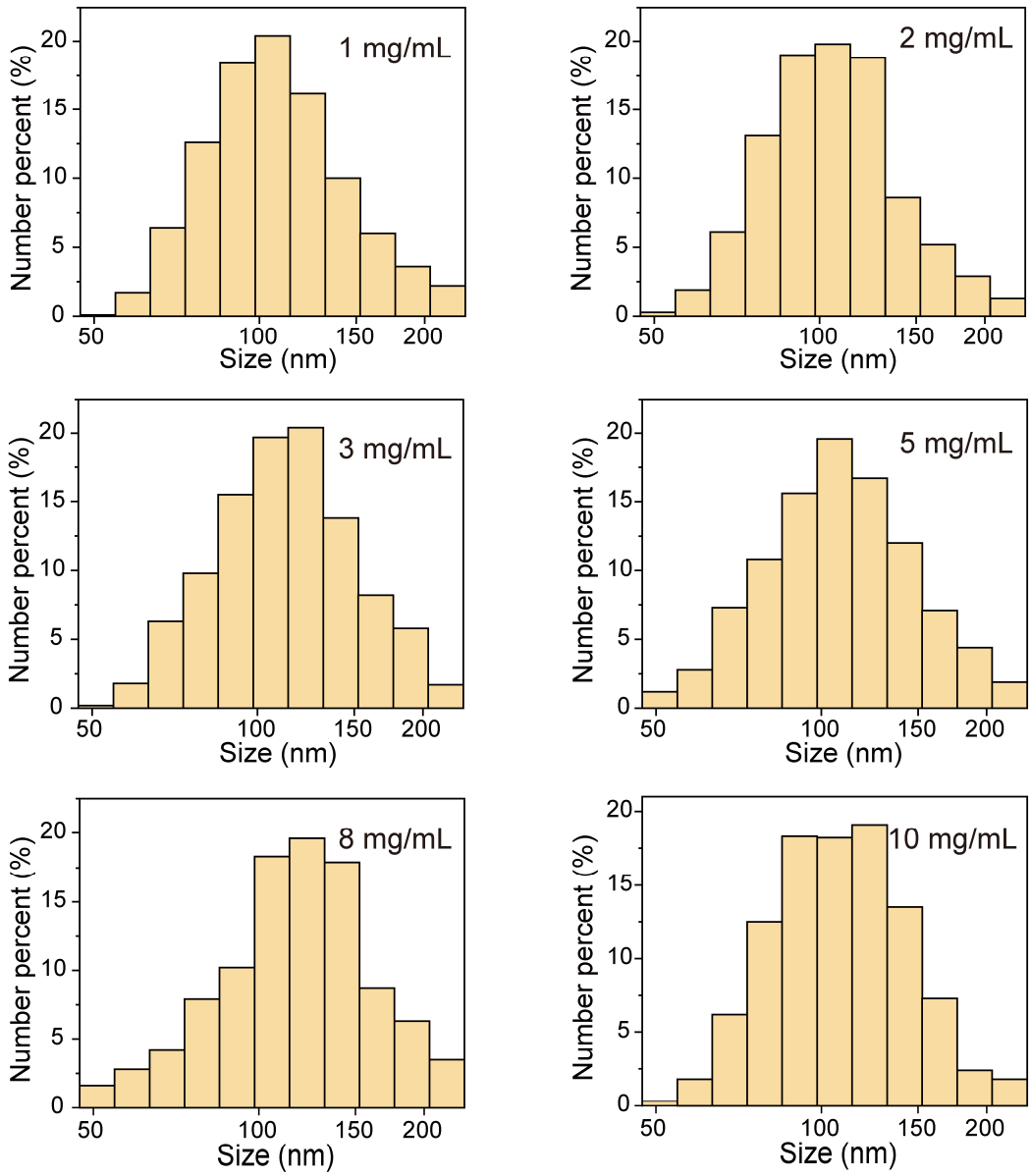


Figure S3. Dynamic light scattering (DLS) number distribution of PdOEP-embedded silica particles.

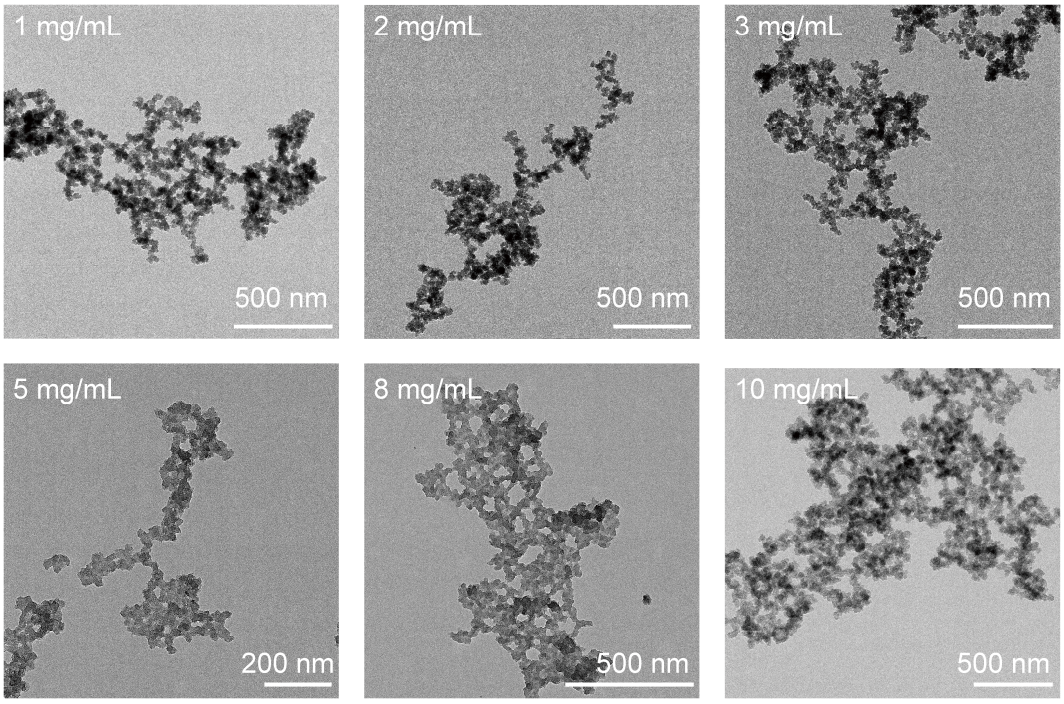


Figure S4. Detailed Transmission electron microscope (TEM) images of PdOEP-embedded silica particles.

Table S1. Relationship between particle size in TEM and surfactant concentration of silica particles.

Concentration of surfactant (mg/mL)	Particle Size (nm)
1	92
2	95
3	91
5	93
8	96
10	97

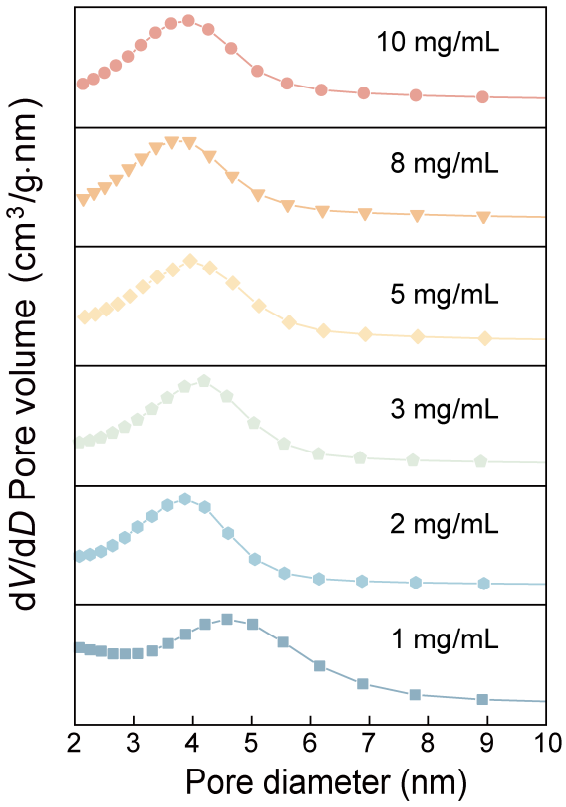


Figure S5. Distribution of pore diameter of PdOEP-embedded silica particles.

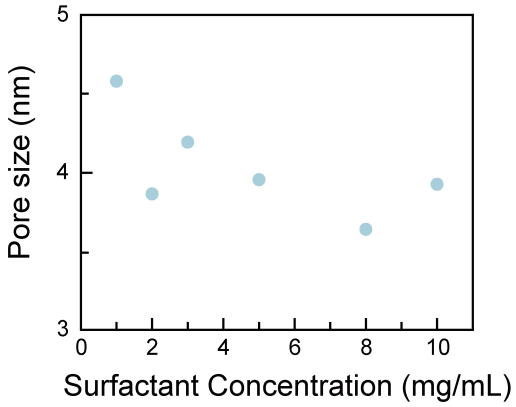


Figure S6. Statistics of pore diameter of PdOEP-embedded silica particles.

The molar concentration of PdOEP molecules within the mesoporous channels was calculated using the following equation, where C represents the embedding capacity of the silica particles, n_{PdOEP} is the initial molar amount of PdOEP, and V_{pore} denotes the mesopore volume.

$$\boldsymbol{c = \frac{C_{dop} \times n_{PdOEP}}{V_{pore}}} \quad \text{(S1)}$$

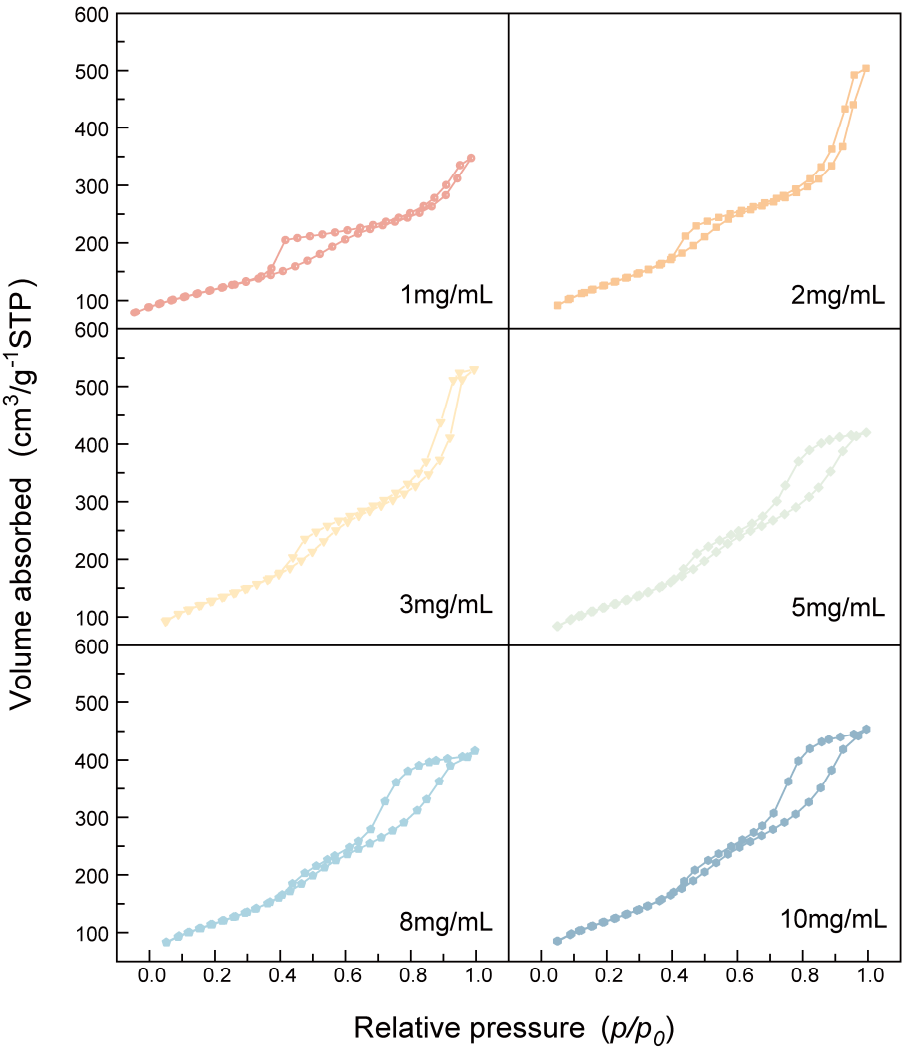


Figure S7. Nitrogen adsorption–desorption isotherms of PdOEP-embedded silica particles prepared at different surfactant concentrations.

Section S3. Spectral characterization of particles and dependence on free volume

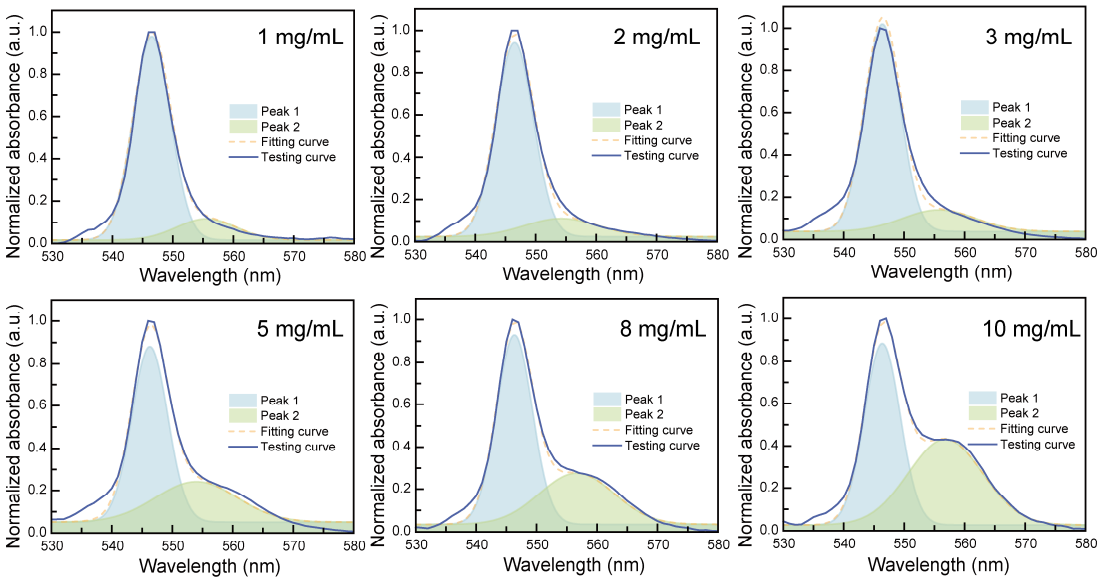


Figure S8. Peak fitting results of Q bands of silica particles with different surfactant concentrations.

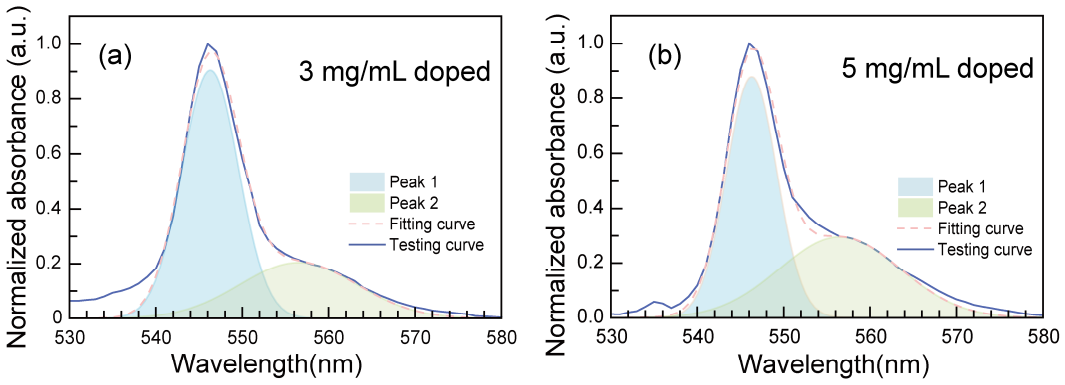


Figure S9. Peak fitting results of Q-band of silica particles with surfactant concentrations of 3mg/mL and 5mg/mL for doped and undoped cholesterol.

Section S4. Experiment on the sensitizing ability of singlet oxygen

The singlet oxygen quantum yield (Φ_Δ) of PdOEP was calculated using the following equation, where r represents the slope of the linear fit of SOSG fluorescence intensity (F_t/F_0) versus irradiation time, which is proportional to the reaction rate between $^1O_2$ and SOSG. A is the absorbance of the sample at 552 nm (the absorption spectra of the silica particles contained scattering signals, which were removed by baseline

correction. The corrected absorption spectra, free from scattering interference, are shown in detail in Figure S13.). In this experiment, Rose Bengal, which has a known singlet oxygen quantum yield of 75% in aqueous solution, was used as the reference photosensitizer. The absorption spectrum and SOSG response of Rose Bengal are shown in Figure S11.

$$\Phi_{\triangle \mathbf{PdOEP}} = \frac{\frac{\boldsymbol{r}_{\mathbf{PdOEP}}}{\boldsymbol{A}_{\mathbf{PdOEP}}}}{\frac{\boldsymbol{r}_{\mathbf{RB}}}{\boldsymbol{A}_{\mathbf{RB}}}} \cdot \Phi_{\triangle \mathbf{RB}} \tag{S2}$$

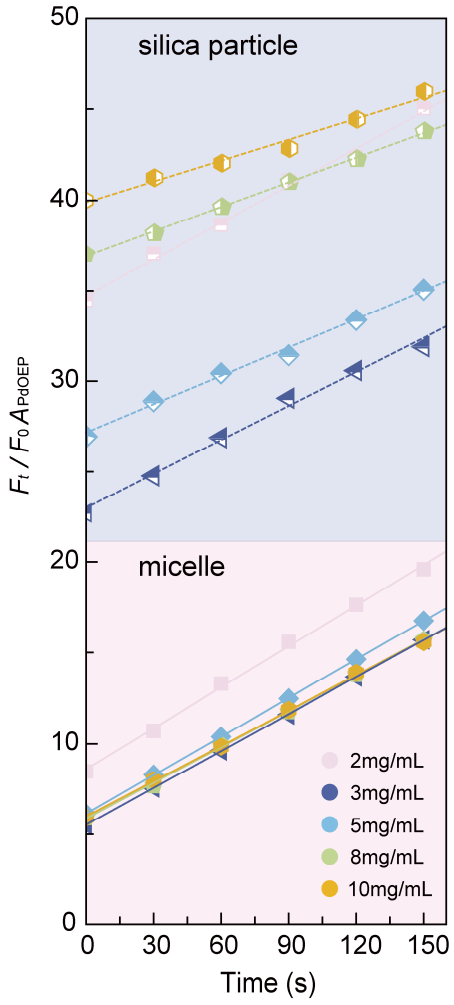


Figure S10. The time-dependent SOSG response of micelle and silica particle samples were recorded under 552 nm excitation to evaluate their singlet oxygen generation behavior.

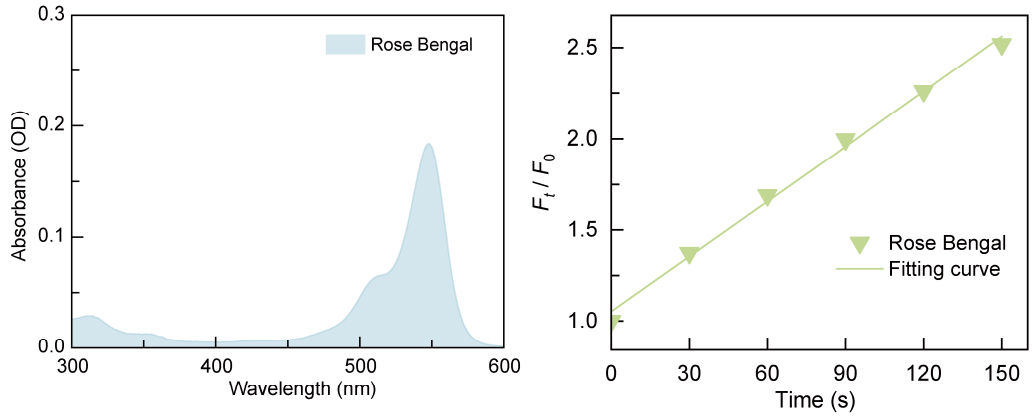


Figure S11. The absorption spectrum of the reference photosensitizer Rose Bengal, as well as its SOSG fluorescence response as a function of irradiation time, were recorded for the determination of singlet oxygen quantum yield.

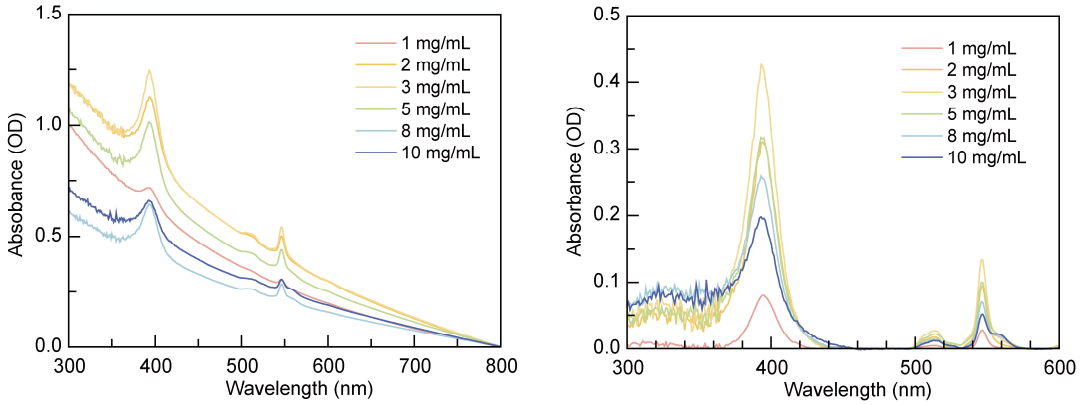


Figure S12. The original and baseline-corrected absorption spectra of PdOEP-embedded silica particles are shown. Due to the extremely low absorbance at 552 nm (~0.007) for silica particles prepared with a surfactant concentration of 1 mg/mL, the resulting error in calculating the singlet oxygen quantum yield would be significant; therefore, this sample was excluded from the analysis. The SOSG fluorescence response of silica particles prepared with a surfactant concentration of 1 mg/mL is shown in Figure S14.

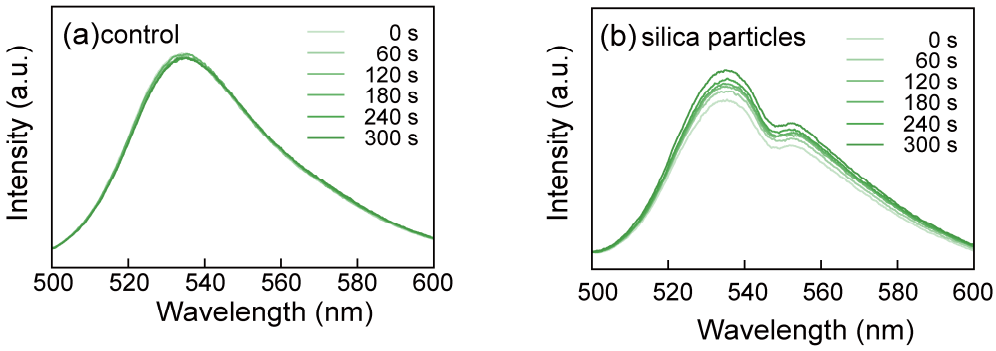


Figure S13. The emission spectrum of SOSG in the two-photon excitation experiment of PdOEP-Tween 80 embedded silica particles.

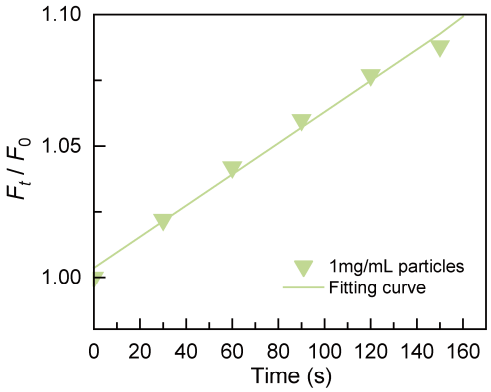


Figure S14. The SOSG fluorescence response of silica particles prepared with a surfactant concentration of 1 mg/mL.